[3]Kumaraswamy, M. P. and Cadambe, V., "Experimental Study of the Vibration of Cantilevered Isoscels Triangular Plates," *Journal of Scientific and Industrial Research* (India), Vol. 15B, No. 2, 1956, pp. 54-60.

[4]Ota, T., Hamada, M., and Tarumoto, T., "Fundamental Frequency of an Isosceles Triangular Plate," *Bulletin of the Japan Society of Mechanical Engineers*, Vol. 4, No. 15, 1961, pp. 478-481.

[5]Williams, R., Yeow, Y. T., and Branson, H. F., "An Analytical and Experimental Study of Vibrating Equilateral Triangular Plates," *SESA Spring Meeting Proceedings*, Chicago, May 1975.

[6]Gustafson, P. N., Stokey, W. F., and Zorowski, C. F., "An Experimental Study of Natural Vibrations of Cantilevered Triangular Plates," *Journal of the Aerospace Sciences*, Vol. 20, 1953, pp. 331-337.

[7]Hewitt, J. S. and Mazumdar, J., "Vibration of Viscoelastic Triangular Plates," *Journal of Engineering Mechanics Division*, ASCE, Vol. 100, No. 6, Dec. 1974, pp. 1143-1146.

[8]Bazeley, G. P., Cheung, Y. K., Irons, B. M., and Zienkiewicz, O. C., "Triangular Elements in Plate Bending-Conforming and Non-Conforming Solutions," *Proceedings of the Conference on Matrix Methods in Structural Mechanics*, WPAFB, Ohio, Oct. 1965, pp. 547-576.

[9]Cowper, G. R., Kosko, E., Lindberg, G. M., and Olson, M. D., "Static and Dynamic Application of High Precision Triangular Plate Bending Elements," *AIAA Journal*, Vol. 7, Oct. 1969, pp. 1957-1965.

Integrated Thermal-Structural Approach for Shells of Revolution

Dennis J. Fallon* and Earl A. Thornton†
Old Dominion University, Norfolk, Virginia

Introduction

THE behavior of shells in severe thermal environments is important in current research on aerospace vehicles. The complex flowfields over missiles and other re-entry vehicles subject their shells to severe aerodynamic heating which requires detailed thermal and structural analyses. Practical shell structures are often analyzed by coupling a finite difference thermal analysis with a finite element structural analysis. Because of basic differences between analytical models an efficient interface is difficult to achieve, and extensive data processing may be required between thermal and structural analyses. The purpose of this Note is to present an integrated thermal-structural analysis for two dimensional shells of revolution. The integrated thermal-structural analysis approach will be considered for thermal prestress effects on aerodynamic instability of shells.

Integrated Finite Element Approach

To more fully develop the potential of the finite element method for thermal-stress analysis the concept of integrated thermal-structural analysis was proposed in Ref. 1. The objectives of the approach are to provide more efficient coupling of the thermal and structural analyses and improve the accuracy of the thermal-stress analysis. The approach is characterized by a common discretization for the thermal and structural analyses utilizing improved thermal elements to predict more detailed temperature variations, and equivalent thermal loads computed with temperature distributions from the improved thermal elements. The key to the approach is the development of new thermal elements which predict more detailed element temperature distributions while maintaining a common discretization with standard structural elements.

The approach used in this Note is to couple a steady-state, one-dimensional thermal finite element analysis with thickness-averaged temperature to a two-dimensional membrane-bending analysis of a shell of revolution. Since shell temperatures are predicted exactly, the thermal prestress effects on the structural response will be considered without loss of accuracy in the structural analysis. The first step in the solution is a thermal analysis whose results can either be nodal temperatures, as in the conventional finite element approach, or a temperature function, as in the integrated finite element approach. In the integrated approach, the results of the thermal analysis are incorporated consistently in a linear structural analysis to obtain thermal prestressing in both the circumferential and meridional direction. Herein lies the difference between the integrated finite element approach and the conventional finite element approach. In the conventional finite element approach the structural analyst is furnished only nodal temperatures from the thermal analysis; hence, the analyst assumes a function (usually linear) to describe the temperature between nodes to perform the necessary integration. However, in integrated finite element analysis there is no need to make this approximation since the actual temperature distribution is furnished from the thermal analysis.

The membrane stress then can be incorporated via the initial (or geometric) stress matrix to evaluate its effects on aerodynamic instability (flutter). This is expressed by the following eigenvalue problem:

$$|[K_e]+[K_g]+\lambda[A_e]-\omega^2[M]|=0 \tag{1}$$

where $[K_e]$ is the linear stiffness matrix, $[K_g]$ the initial stress matrix, $[A_e]$ the aerodynamic matrix, $[M]$ the mass matrix, λ the aerodynamic coefficient, and ω the natural frequency.

Finite Element Modeling

The exact thermal finite element formulation is based on conservation of energy for a shell of revolution. For axisymmetric conditions the energy equation has the general form[2]

$$\frac{d}{ds}\left[P(s)\frac{dT}{ds}\right]+Q(s)T=R(s) \tag{2}$$

where the temperature T is a function of the meridional coordinate s. Equation (2) may combine conduction with convection, internal heat generation, or surface heating.

Exact interpolation functions for the finite element formulation of Eq. (2) can be derived from the general solution to the differential equation. By imposing the temperature boundary condition at each end of the element, a finite element interpolation function can be formulated in terms of the meridional coordinate, the end temperatures T_1 and T_2, and a nodeless parameter T_0. An element's temperature interpolation function is written as[2]

$$T(s)=N_0(s)T_0+N_1(s)T_1+N_2(s)T_2 \tag{3}$$

Element interpolation functions derived in the form of Eq. (3) are not generally the same as used in conventional finite elements since they result from the differential-equation solution. These functions may be simple polynomials or transcendental functions depending on the solution of Eq. (2). Exact expressions for the temperature interpolation functions used in this Note are tabulated in Ref. 2.

For the structural analysis, a geometrically exact shell element with seven degrees of freedom per nodal circle is employed. The interpolation functions for this element are expressed as a Fourier series in the circumferential direction

Presented as Paper 82-0701 at the AIAA/ASME/ASCE/AHS 23rd Structures, Structural Dynamics and Materials Conference, New Orleans, La., May 10-12, 1982; submitted May 12, 1982; revision received Dec. 7, 1982.

*Assistant Professor, Civil Engineering Department.
†Professor, Mechanical Engineering and Mechanics Department.

and simple polynomials in the meridional direction. The interpolation functions are

$$u=\sum_{n=0} u_n(s)\cos n\theta,\quad v=\sum_{n=0} v_n(s)\sin n\theta,\quad w=\sum_{n=0} w_n(s)\cos n\theta \tag{4}$$

where u, v, and w represent displacements in the meridional, circumferential, and normal directions, respectively; u_n, v_n, and w_n are simple polynomials of the meridional coordinate s; and θ is the circumferential coordinate.

The linear stiffness matrix defined in Eq. (1) can be derived from the minimization of the first-order strain energy equation.[3] The consistent initial stress matrix which incorporates the effects of thermal prestressing is formulated from the contributions of the second-order strains in the strain energy expression.[4] The thermal prestressing is obtained in the classical manner[5] using the exact interpolation function as expressed by Eq. (3) in the integrated finite element approach or a linear function in the conventional finite element approach. The consistent mass matrix is derived from the kinetic energy of the system[3] and the aerodynamic matrix is derived from the virtual work of the aerodynamic forces assuming a first-order high Mach number approximation to linear potential flow theory.[6] Aerodynamic damping which has been shown to have very small effect on the critical flutter boundary[7] is neglected.

Flutter Analysis

The objective of an aerodynamic instability analysis is to seek a set of vibration modes that are unbounded in the time domain. This criteria is achieved when the natural frequencies ω are complex quantities. When $\lambda=0$ in Eq. (1) the problem degenerates into the calculation of the in-vacuo natural frequencies of the free vibration case. As λ is increased from zero, two of the eigenvalues approach each other and coalesce at a critical value of λ designated λ_{cr}. As the value of λ is increased beyond λ_{cr} the eigenvalues become complex conjugates. By using the interpolation functions defined in Eq. (4), the analysis of shells reduces to seeking solutions of Eq. (1) for each harmonic. To obtain a complete solution to a given shell, all harmonics must be searched to determine the lowest value for λ.

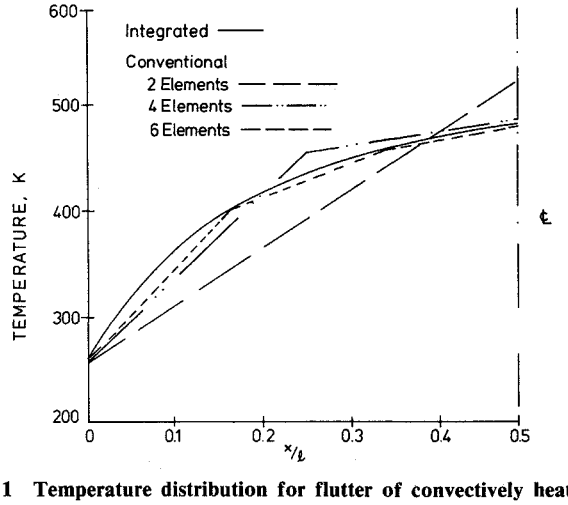

Fig. 1 Temperature distribution for flutter of convectively heated shell.

Table 1 Comparison of meridional forces and critical aerodynamic factor

No. of Elements	Conventional N_s[a]	Conventional λ[b]	Integrated N_s	Integrated λ
2	0.823	38.0	1.033	6.0
4	0.981	10.2	1.020	8.9
6	1.000	9.1	1.016	9.0

[a] N_s = meridional force in MN/m. [b] λ = critical aerodynamic coefficient.

Numerical Results

To demonstrate the integrated finite element approach, a cylindrical steel shell was subjected to convective heating. The ambient temperature was assumed to be 480 K and the ends are held at a temperature of 255 K. The shell is 1.219-m long with a radius and thickness of 40.6 cm and 2.54 mm, respectively. The boundary conditions for the structural analysis are simple supports.

The results from the thermal, thermal stress, and aerodynamic analyses for the integrated finite element approach and conventional approach using two, four, and six elements are illustrated in Fig. 1 and Table 1. Using only two elements the conventional approach gives a poor approximation to the exact temperature distribution determined from the integrated finite element approach. As a consequence, the meridional forces in the shell computed from the two temperature distributions differ by approximately 30%. This leads to a significant difference in the critical aerodynamic factor. Using four elements gives a much better approximation to the exact temperature distribution, and differences between predictions for the meridional force and critical aerodynamic factor are much improved. The conventional approach using six elements provides an excellent approximation to the exact temperature distribution. Hence, there is very good agreement for the meridional force and the critical aerodynamic factor.

Concluding Remarks

An example of aerodynamic instability (flutter) calculations is presented to illustrate the accuracy of the shell element and the integrated thermal-structural analysis approach. The effects of the temperature distribution on meridional force and critical aerodynamic factor for a cylindrical shell were studied for temperatures computed by conventional thermal elements and exact thermal elements. The results demonstrated the importance of accurately computing shell temperature distributions and integrating these distributions consistently in the structural analysis.

Acknowledgment

This work was funded by NASA Langley Research Center under Grant NSG 1167.

References

[1] Thornton, E. A., Dechaumphai, P., and Wieting, A. R., "Integrated Thermal-Structural Finite Element Analysis," AIAA Paper 80-0717, *Proceedings of the AIAA/ASME/ASCE/AHS 21st Structures, Structural Dynamics, and Materials Conference*, Seattle, Wash., May 1980.

[2] Thornton, E. A., Dechaumphai, P., and Tamma, K. K., "Exact Finite Elements for Conduction and Convection," Second International Conference on Numerical Methods in Thermal Problems, Venice, Italy, July 1981.

[3] Adelman, H. M., Catherines, D. S., and Walton, W. C., "A Method for Computation of Vibration Modes and Frequencies of Orthotropic Thin Shells of Revolution Having General Meridional Curvature," NASA TN D4972, Jan. 1969.

[4] Lashkari, M., Weingenten, V. I., and Margoleas, D. S., "Vibration of Pressure Loaded Hyperbolic Shells," *Journal of Engineering Mechanics Division*, ASCE, Vol. 98, Oct. 1972, pp. 1017-1030.

[5]Adelman, H. M., Lester, H. C., and Rogers, J. L., "A Finite Element for Thermal Stress Analysis of Shells of Revolution," NASA TN D7286, Dec. 1973.
[6]Bismarck-Nasr, M. N., "Finite Element Method Applied to Supersonic Flutter of Circular Cylindrical Shells," *International Journal for Numerical Methods in Engineering*, Vol. 10, No. 1, 1976, pp. 423-435.
[7]Dixon, S. C. and Hudson, M. L., "Flutter, Vibration and Buckling of Truncated Orthotropic Conical Shells with Generalized Elastic Edge Restraint, NASA TN D-5759, July 1970.

Inelastic Buckling of Cylindrical Shells Subjected to Axial Tension and External Pressure

N. C. Huang*
University of Notre Dame, Notre Dame, Indiana
and
P. D. Pattillo†
Amoco Production Company, Tulsa, Oklahoma

Introduction

In the collapse design of oil well casing, the casing is always modeled as having infinite length. Inasmuch as the length/diameter ratio of a typical field joint will vary from 18 to 80, this assumption is reasonable. However, the experimental fixtures from which full-scale collapse data is obtained in steel mills will only accommodate samples having length/diameter ratios in the range of 2-8. The question therefore arises as to by what means experimental results on cylinders of finite length may be translated into design values for longer cylinders. In a recent empirical study of collapse without axial load, Clinedinst[1] has concluded that a length/diameter ratio of 8 is sufficient for the casing to be considered infinite. However, this conclusion is based entirely on 1) analysis of short samples (the largest length/diameter ratio reported was 6:1), and 2) no end constraints. There is currently no method of relating full-scale tests with axial load and clamped end conditions to the behavior of a joint of infinite length. The aim of this analysis is to present specific guidelines by which one can account for the length of the specimen and thereby predict the length/diameter ratio beyond which the effect of the boundary region at the edge of the casing becomes inconsequential.

Analysis

Consider a circular cylindrical shell of length L, mean radius R, and thickness h. The shell is subjected to an axial tensile stress f and an external hydrostatic pressure P on the curved surface measured per unit area of the midsurface. We now introduce the following dimensionless quantities:

$$\lambda=\frac{h}{R},\quad d=\frac{L}{2R},\quad p=\frac{PR}{Eh},\quad \bar{f}=\frac{f}{E},\quad \tau_e=\frac{\sigma_e}{E} \tag{1}$$

where σ_e is the effective stress and E the elastic modulus of the material.

Our analysis is based on Sanders' nonlinear shell equations.[2] The rotations about the normal to the midsurface are neglected. The strain components at any point in the shell are related to the membrane strains and curvatures of the midsurface by relations given by Novozhilov.[3] We shall consider only small strains. The material is considered to be elastic-plastic. Both the J_2-incremental theory and the J_2-deformation theory are employed in the formulation. The material constants used in the constitutive relations are derived from the conversion of the relation of the effective stress and the effective strain which is determined from a uniaxial tension test, or an appropriate model of uniaxial stress-strain behavior such as Needleman's curve.[4] The membrane forces and moments are related to the stresses in the shell by integrations through the shell thickness. Since the deformation is symmetric with respect to the midlength, only half of the shell need be considered. All boundary conditions are derived based on Sanders' consistent theory.[2] At the ends of the shell we consider the shell to be clamped.

Prior to buckling the deformation of the shell is axisymmetric. In this case, all physical and geometric quantities are independent of the polar angle. The governing differential equations and boundary conditions for the prebuckling deformation can be derived easily. The calculation of the prebuckling deformation is based on a finite difference scheme with an iterative procedure, i.e., in each incremental step a condition of either loading or unloading is assumed. Two types of loading are considered: proportional loading and constant axial loading. In the latter case, the value of τ_e is checked at each step. When τ_e exceeds a critical value $(\tau_e)_c$, the shell collapses due to exceeding the ultimate strength rather than bifurcation.

In the plastic buckling analysis, the additional physical and geometric quantities introduced by buckling are expressed as sinusoidal functions of the polar angle and the wave number n in the transverse direction. Since our interest lies in finding the critical condition for buckling, second-order terms are neglected. An eigenvalue problem can be formulated. The critical condition for buckling is determined by the characteristic equation of the eigenvalue problem. The value of n corresponding to the lowest load at which buckling occurs will determine the shape of the buckling mode. The details of the analysis are given in Ref. 5.

Numerical Results and Discussion

As pointed out in the introduction, the practical impetus for this study was to obtain a relation between the collapse behavior of short tubes and the collapse behavior of tubes that are essentially infinite in length. However, prior to investigating the effect of length/diameter ratio on collapse behavior, it is instructive to begin with a comparison of the two plasticity theories carried throughout the development. Figure 1 is a plot of predicted dimensionless collapse resistance as a function of axial tension for a cylinder with fixed ends. The collapse predictions are compared to data from Edwards and Miller[6] on small tubes with dimensions $\lambda=0.1227$, $d=16.54$, and a uniaxial stress-strain curve (τ-e curve) that may be fit with Needleman's model

$$\tau/\tau_y=\begin{cases} e/e_y & \text{for } e\le e_y \\ [m(e/e_y)+1-m]^{1/m} & \text{for } e>e_y \end{cases} \tag{2}$$

using $\tau_y=1.679\times10^{-3}$ and $m=5.0$, where τ_y is the dimensionless proportional limit normalized with respect to the modulus of elasticity and e_y is the corresponding strain. Poisson's ratio of the material is considered to be 0.3. The two curves in the figure are labeled by a pair of letters indicating the particular plasticity theory used in analyzing 1) the prebuckled configuration and 2) bifurcation from the fundamental state. For example, the designation I-D indicates that the incremental theory of plasticity (I) was used to determine the prebuckled configuration and the deformation theory of plasticity (D) was used in the buckling analysis.

Received Aug. 16, 1982; revision received Dec. 13, 1982.

*Professor, Department of Aerospace and Mechanical Engineering.
†Research Associate.